Raman study of Li$_{1-x}$H$_x$IO$_3$ crystals

M A Pimenta†, M A S Oliveira†, P Bourson‡ and J M Crettez§

† Departamento de Fisica, Universidade Federal de Minas Gerais, Caixa Postal 702, 30123-970 Belo Horizonte, Brazil‖

‡ Laboratoire Matériaux Optiques à Propriétés Spécifiques, CLOES Université de Metz and Supelec, 2 rue E Belin, 57078 Metz Cédex 3, France

§ Laboratoire de Physique de l'Université de Bourgogne, CNRS/UPRES A 5027, Faculté des Sciences, BP 138, 21004 Dijon Cédex, France

Abstract. In this work we present a polarized Raman study of Li$_{1-x}$H$_x$IO$_3$ single crystals for several values of the concentration x ($x \leqslant 0.36$) made using different scattering geometries. The Raman spectra, composed of broad bands, have been fitted in accordance with a symmetry analysis which allowed us to assign the vibrational modes, and determine their frequencies and damping constants. The results are compatible with an average hexagonal symmetry for the solid solutions with x in the range $0.27 \leqslant x \leqslant 0.36$. In each of the spectra we found two bands at about 590 and 730 cm^{-1}, probably associated with the existence of O–H...O structures in the solid solutions.

1. Introduction

Raman scattering is a very useful tool for studying the lattice dynamics of disordered crystals. Strictly speaking, these crystals do not present a unit cell that repeats periodically in the three-dimensional space, and, therefore, the Raman spectra would reflect a density of vibrational states. However, in general, the Raman bands associated with the vibrational modes are not so wide, and some kind of selection rule for the Raman scattering remains.

The Raman spectrum of disordered systems of the type A$_{1-x}$B$_x$C can be roughly classified into three types. In a very simple case, it varies continuously from the spectrum of the AC to that of the BC compound. In other systems, the Raman spectrum is constituted by the superposition of the spectra of the AC and BC compounds, the relative intensity of each one being proportional to the concentration x. However, a more complicated situation occurs when the structures of the pure compounds AC and BC are quite different. The Raman spectrum can be different from those of the pure compounds in some regions of the phase diagram, presenting in this case broad bands typical of amorphous compounds.

This third situation occurs in the case of Li$_{1-x}$H$_x$IO$_3$ crystals. In 1951, Ricci and Amron [1] studied the phase diagram of the aqueous system containing iodic acid (HIO$_3$) and lithium iodate (LiIO$_3$), and they observed that a solid solution of the type Li$_{1-x}$H$_x$IO$_3$ crystallizes for x ranging between approximately 0.22 and 0.36. In the other regions of the phase diagram, they observed the mixture of this solid solution and the pure compounds. This solid solution has been well studied over recent years, principally because its structure is very close to

‖ E-mail: mpimenta@fisica.ufmg.br

that of lithium iodate ($LiIO_3$), a crystal that presents interesting physical properties (high non-linear optical coefficients, high piezoelectric coefficients, ionic conductivity, etc).

The room temperature structures of the pure compounds HIO_3 and $LiIO_3$ are quite different. The stable non-centrosymmetric form of lithium iodate (α-$LiIO_3$) presents a hexagonal symmetry, belonging to the space group $P6_3$, with two formulae per unit cell [2]. The lithium ions occupy the Wyckoff positions a, forming a hexagonal framework, and all of the pyramidal iodate anions point along the c-direction and occupy the Wyckoff positions b. The room temperature structure of the iodic acid (α-HIO_3) belongs to the orthorhombic space group $P2_12_12_1$ with four formulae per unit cell [3]. The IO_3^- pyramids are not regular (the distances between the iodine and the three oxygen atoms are not the same), and are oriented along four different directions in the unit cell. The protons form hydrogen bonds between oxygen atoms belonging to different IO_3^- anions, and all of the atoms occupy general positions in the unit cell.
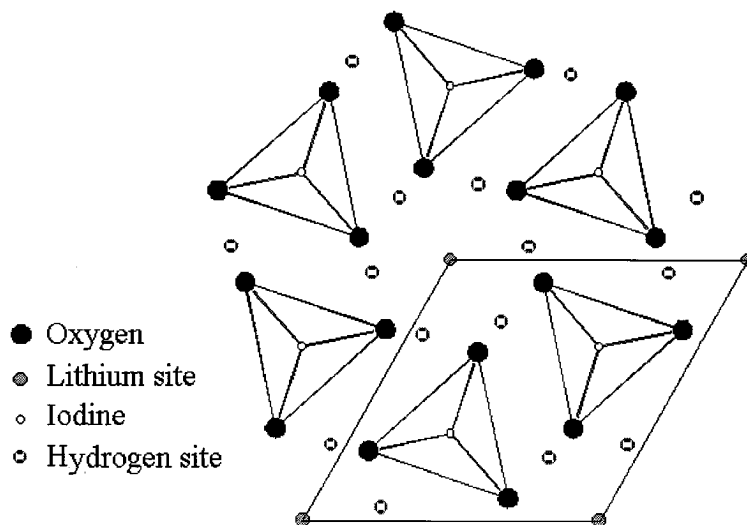
Figure 1. The crystal structure of $Li_{1-x}H_xIO_3$ ($x \approx 0.33$) projected onto the basal plane. The protons do not replace the lithium ions, but are randomly distributed in general positions between two oxygen atoms belonging to different iodate groups, with an occupation factor of 0.33.

In a first tentative description of the symmetry of $Li_{1-x}H_xIO_3$ crystals in the concentration range 0.22–0.36, Hamid and Kunze [4] showed that the factor group analysis used to describe the IR and Raman data of α-$LiIO_3$ could not be applied to these solid solutions. Avdienko *et al* [5], ascertained, with the support of their Raman results, that the structure and symmetry of $Li_{1-x}H_xIO_3$ crystals would be different from those of α-$LiIO_3$ and α-HIO_3. Barabash *et al* [6] performed a Raman study of polycrystalline samples of $Li_{1-x}H_xIO_3$ over a wide range of concentration x, and observed that the Raman spectra in the range 0.22–0.36 were composed of anomalous broad bands, characteristic of disordered crystals. It was shown in this study that the Raman spectra of solid solutions for $x > 0.36$ corresponded to the superposition of this broad-band spectrum with that of α-HIO_3 crystal. These authors also performed a polarized Raman study of a $Li_{1-x}H_xIO_3$ ($x = 0.30$) single crystal, and they showed that the Raman spectra obtained using the (zy) and (yx) polarization geometries were practically the same. This result led them to conclude that the solid solutions could not be isomorphous with α-$LiIO_3$. However, in 1990, Le Roy *et al*

[7] determined the room temperature structure of Li$_{1-x}$H$_x$IO$_3$ ($x = 0.33$) by x-ray single-crystal and neutron powder diffraction, and concluded that it presents a hexagonal average symmetry, belonging to the same C$_6^6$ ($P6_3$) space group as α-LiIO$_3$. Figure 1 shows the crystal structure of the hydrated solid solution as determined in reference [7]. Note that the protons do not replace the lithium ions, but are randomly distributed in general positions between two oxygen atoms belonging to different iodate groups, with an occupation factor of 0.33. The precise localization of protons established by single-crystal neutron diffraction has been published recently [8]. In a neutron powder diffraction study of the Li$_{1-x}$H$_x$IO$_3$ ($x = 0.33$) solid solution at high temperature, Bouillot *et al* [9] observed a decrease of the proton concentration when the samples were heated above 125 °C. They also observed that the protons escaped from the sample above approximately 235 °C.

In order to elucidate why the previous Raman studies [5, 6] and the neutron and x-ray results [7] are at variance, a complete polarized Raman study of Li$_{1-x}$H$_x$IO$_3$ single crystals for several values of x ($x \leqslant 0.36$) was performed, using different scattering geometries. The results and their analysis are presented in the following.

2. Experimental procedure

Single crystals of Li$_{1-x}$H$_x$IO$_3$ have been grown by slow evaporation of saturated aqueous solutions containing LiIO$_3$ and HIO$_3$ in several molar ratios. Crystals of good optical quality were obtained with dimensions of about $2 \times 2 \times 5$ mm. The concentration x of protons in each sample was obtained from the determination of the lattice parameters c and a, using the relation proposed by Le Roy *et al* [7], which relates x to the ratio c/a. The coordinate system used in the Raman experiments is such that z is the hexagonal axis, x is perpendicular to z and parallel to a natural face of the crystal, and y is perpendicular to x and z.

The Raman spectra have been taken using a triple-monochromator spectrometer (DILOR XY) equipped with a multi-array detector (GOLD). A microscope (OLYMPUS BH-2) is coupled to the spectrometer, allowing a Raman analysis with a lateral spatial resolution of about 2 μm and a deep resolution of about 5 μm (the micro-Raman technique). We have used an argon laser (COHERENT INNOVA 70), operating with the green line ($\lambda = 514.5$ nm), and the laser power was about 200 mW. Both the micro- and macro-entrances of the spectrometer were used to perform the measurements, and the spectra obtained were identical. The time for recording a spectrum was about 1 min, and no damage of the sample surface was observed.

3. Results and discussion

Figure 2 shows the Raman spectra at room temperature of the Li$_{1-x}$H$_x$IO$_3$ crystals for several values of the concentration x obtained using the $Y(XX)\bar{Y}$ scattering geometry, compared with the spectrum of the pure compound LiIO$_3$. The Bose factor ($n(\omega)+1$) was divided out of all of the spectra presented in this study. It is interesting to observe that the spectrum of the solid solution with low H$^+$ concentration ($x = 0.06$) is very similar to that of the pure compound LiIO$_3$. This low concentration value was roughly estimated from a dielectric behaviour, which is strongly dependent on this parameter [10]. The spectrum is composed of sharp peaks associated with internal modes of the IO$_3^-$ anion (the symmetrical (ν_1) and anti-symmetrical (ν_3) stretching modes at around 800 cm^{-1} and the symmetrical (ν_2) and anti-symmetrical (ν_4) bending modes between 340 and 500 cm^{-1}) and peaks associated with

the external modes localized below 340 cm^{-1}. Detailed discussions of mode assignment for pure α-LiIO$_3$ may be found in references [11] and [12]. The spectra of the solid solutions for $x \geqslant 0.27$ are quite different. Firstly, note the broadening of all of the bands with respect to those of the pure LiIO$_3$ compound. Another important feature observed in figure 2 is the appearance of two bands localized at 590 and 730 cm^{-1}, whose intensities and widths increase with increasing H$^+$ concentration. It is also interesting to observe that the intensity of the peaks below 200 cm^{-1} increases with increasing x.
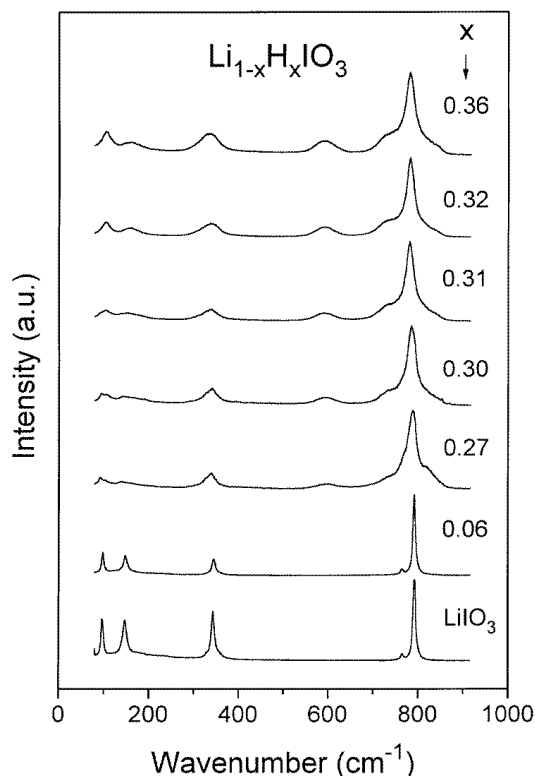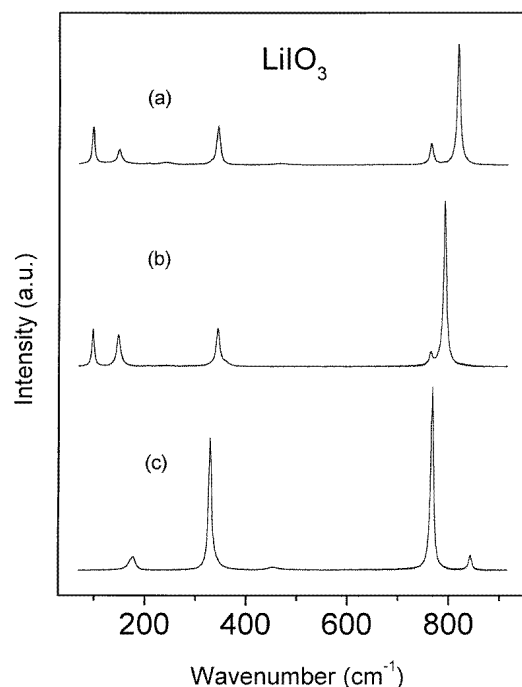

Figure 2. Raman spectra of Li$_{1-x}$H$_x$IO$_3$ single crystals in the $Y(XX)\bar{Y}$ scattering configuration for several values of the proton concentration x, including the case where $x = 0$ in the lower part.

In figure 3, the Raman spectra of the crystal with $x = 0.32$ obtained using three different scattering configurations, namely, $Z(XX)\bar{Z}$, $Y(XX)\bar{Y}$ and $Y(XZ)\bar{Y}$, are shown in detail. The spectra obtained with the $Z(XY)\bar{Z}$ scattering geometry (not shown in this figure) are very similar to those of the $Z(XX)\bar{Z}$ geometry, which display E$_2$ and A(LO) symmetry modes. In fact, we would expect to find only the E$_2$ symmetry modes when using the $Z(XY)\bar{Z}$ scattering geometry. The observation of A(LO) modes in this geometry is probably due to a slight crystal misorientation. The spectra of the solid solutions with different x-concentrations ($0.27 \leqslant x \leqslant 0.36$) are quite similar to the $x = 0.32$ one, with the exception of the bands at about 590 and 730 cm^{-1} which increase and widen with increasing x.

A series of measurements were performed after turning the sample by 60° around the c-axis. The results obtained using different scattering geometries were found to be absolutely
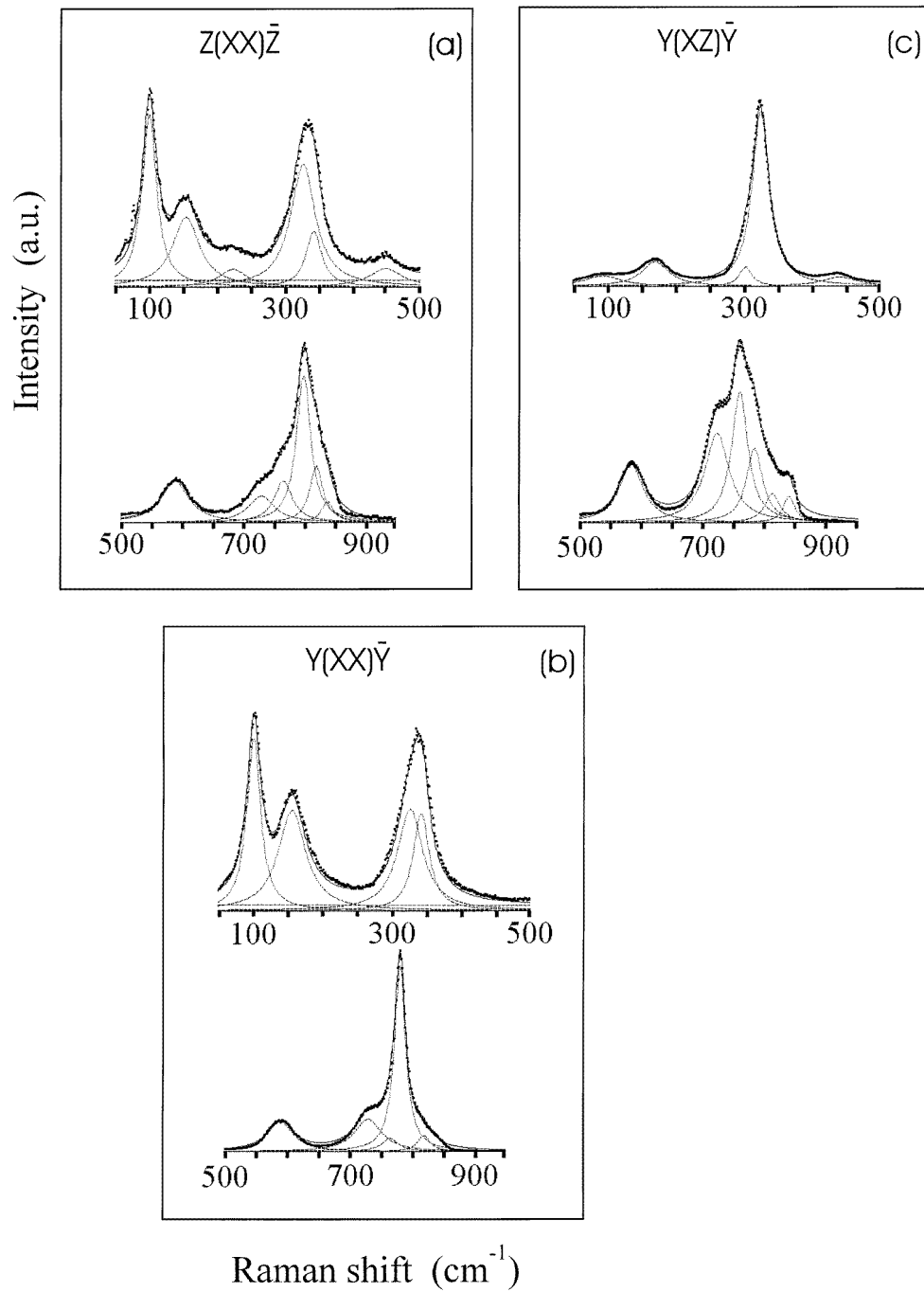
Figure 3. Raman spectra of the $Li_{1-x}H_xIO_3$ ($x = 0.32$) single crystal in three scattering configurations. The Lorentzian components are shown below the observed profile. (a) $Z(XX)\bar{Z}$, (b) $Y(XX)\bar{Y}$ and (c) $Y(XZ)\bar{Y}$. The Bose factor $n(\omega) + 1$ was divided out of the spectra.
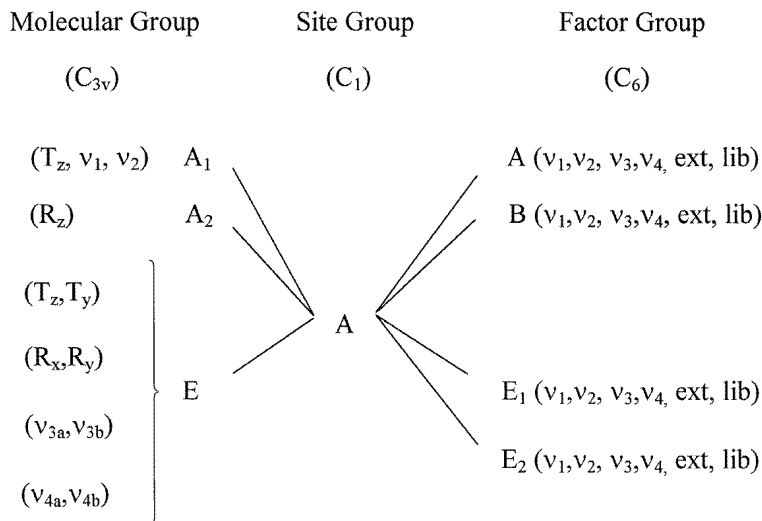
Figure 4. Raman spectra of the pure $LiIO_3$ single crystal in three scattering configurations. (a) $Z(XX)\bar{Z}$, (b) $Y(XX)\bar{Y}$, and (c) $Y(XZ)\bar{Y}$.

invariant under this symmetry operation, in accordance with the x-ray and neutron results [7], which proposed a hexagonal symmetry structure.

Le Roy *et al* [7] showed that the $Li_{1-x}H_xIO_3$ crystals with x in the interval $0.22 < x < 0.36$ present a hexagonal symmetry, belonging to the same C_6^6 ($P6_3$) space group as the α-$LiIO_3$ crystal. In the case of the pure compound $LiIO_3$, the IO_3^- pyramidal anions occupy C_3 sites (Wyckoff position b), and a correlation analysis shows that the internal modes ν_1 and ν_2 of the iodate anion belong to the A and B irreducible representations and the internal modes ν_1 and ν_2 belong to the E_1 and E_2 representations of the C_6 point group [13]. The B-symmetry modes are not Raman active, and will be not considered in the following analysis. Figure 4 shows the Raman spectra of the pure $LiIO_3$ taken under the same experimental conditions as were used to obtain figure 3. In the polarized Raman spectrum of $LiIO_3$ obtained using the $Z(XX)\bar{Z}$ scattering geometry (figure 4(a)), we observe the longitudinal (LO) modes ν_1 (817 cm^{-1}) and ν_2 (468 cm^{-1}) belonging to the A irreducible representation and the modes ν_3 (765 cm^{-1}) and ν_4 (324 cm^{-1}) belonging to E_2. The transverse (TO) modes ν_1 (795 cm^{-1}) and ν_2 (358 cm^{-1}) belonging to A, and, again, the modes ν_3 and ν_4 belonging to E_2 appear in the $Y(XX)\bar{Y}$ spectrum (figure 4(b)). The transverse and longitudinal (TO and LO) modes ν_3 (769–848 cm^{-1}) and ν_4 (450–460 cm^{-1}) belonging to E_1 are observed in the $Y(XZ)\bar{Y}$ scattering geometry (figure 4(c)). The peaks at lower frequencies are associated with the external modes.

The selection rules discussed above for the $LiIO_3$ pure crystal are no longer valid for the case of $Li_{1-x}H_xIO_3$ crystals, in spite of the fact that they share the same C_6^6 ($P6_3$) space group. Strictly speaking, these solid solutions do not have a unit cell which repeats periodically in three dimensions. Also, the random presence of protons and lithium vacancies breaks the threefold symmetry of the iodate anion sites. Moreover, the protons present in the structure are localized between oxygen atoms belonging to different iodate anions, and certainly they provoke a distortion of the regular pyramidal form of these

Molecular Group	Site Group	Factor Group
(C$_{3v}$)	(C$_1$)	(C$_6$)

(T$_z$, ν$_1$, ν$_2$)　A$_1$

(R$_z$)　A$_2$

(T$_z$,T$_y$)

(R$_x$,R$_y$)

(ν$_{3a}$,ν$_{3b}$)　E

(ν$_{4a}$,ν$_{4b}$)

A

A (ν$_1$,ν$_2$, ν$_3$,ν$_4$, ext, lib)

B (ν$_1$,ν$_2$, ν$_3$,ν$_4$, ext, lib)

E$_1$ (ν$_1$,ν$_2$, ν$_3$,ν$_4$, ext, lib)

E$_2$ (ν$_1$,ν$_2$, ν$_3$,ν$_4$, ext, lib)

Figure 5. The correlation diagram for the internal modes of the iodate anion in Li$_{1-x}$H$_x$IO$_3$ crystals ($0.27 \leqslant x \leqslant 0.36$).

anions. Nevertheless, the spectra shown in figure 3 are clearly dependent of the scattering geometry used, suggesting that some kind of selection rule must be obeyed. This result is in contradiction with a previous Raman study [6], in which it was suggested that the Raman spectra of the solid solutions obtained using different scattering geometries were similar.

A group theoretical analysis predicting the number of Raman-active modes cannot be performed in the case of the solid solutions, due to the random partial occupation of the sites. Nevertheless, some symmetry considerations can be used in order to analyse their Raman spectra. As already emphasized, there are several different kinds of iodate anion, each one with different surroundings and distortions. We can consider the IO$_3^-$ ions to be localized in sites with C$_1$ symmetry. Figure 5 shows a correlation diagram, which correlates the point group of the free IO$_3^-$ ions (C$_{3v}$), the site group (C$_1$), and the factor group of the crystal (C$_6$). Note that this is a qualitative diagram, since it does not predict the number of internal modes associated with each representation. According to this diagram, we must expect the presence of four types of internal mode ($ν_1$, $ν_2$, $ν_3$ and $ν_4$), belonging to each irreducible representation of the C$_6$ point group. Each internal mode gives rise to a relatively broad peak in the Raman spectra, which corresponds to the superposition of single peaks associated with the different kinds of iodate anion. Note that in the case of the pure compound LiIO$_3$, the modes $ν_1$ and $ν_2$ have A symmetry, and the modes $ν_3$ and $ν_4$ have E$_1$ or E$_2$ symmetry.

The Raman spectra shown in figure 3 were then fitted by a sum of Lorentzian lines, in accordance with the analysis discussed above. It must be emphasized that, in general, a great number of parameters were used to fit these broad bands, and, therefore, there were several different sets of parameters which fitted such bands equally well. We have therefore to introduce some restrictions in the fitting procedure, in order to achieve a good fit with a physical meaning. Firstly, we considered the constraints related to the crystal symmetry. For example, the E$_2$-symmetry modes must appear in both spectra obtained using the $Y(XX)\bar{Y}$ and $Z(XX)\bar{Z}$ geometries with the same frequencies and damping constants. Also, the LO modes must have their frequencies greater than (or almost equal to) the TO counterpart, the TO–LO splitting being proportional to the polar character of the mode (with the exception

of a particular case that will be discussed later). Moreover, the frequencies used to fit the spectra and the attributions of the vibrational modes were always compatible with those of the pure compound $LiIO_3$ [11–14].

Another restriction on the set of fitting parameters concerned the coherence of the fittings for the spectra of different samples obtained using the same scattering geometry. The procedure adopted was to fix the frequencies and damping constants of the vibrational modes for the samples with different concentrations x ($0.27 < x < 0.36$). The spectra for different samples obtained with the same scattering geometry have been fitted using practically the same set of frequencies and damping constants. The only exception concerned the damping constants of the modes at about 590 and 730 cm^{-1}. It was observed that the damping constants of these two modes increased with increasing concentration x.

In order to investigate the influence of the protons on the lattice dynamics of the $Li_{1-x}H_xIO_3$ crystals, we have performed a thermal treatment of the samples, since it was observed that the protons escape from the host lattice at high temperature [9]. This thermal treatment consisted in keeping the sample with $x = 0.32$ at 150 °C for 24 hours in a vacuum of 10^{-2} mbar. We observed the disappearance of the bands localized at about 590 and 730 cm^{-1} in the spectra obtained after the thermal treatment, at room temperature, by focusing the laser beam on the surface of the sample. This result allowed us to conclude that these bands are certainly associated with the presence of the protons in the lattice. Turrel [15] showed that, in compounds with hydrogen bonds, there are stretching and torsional modes of the X–H...Y structures whose frequencies are compatible with those discussed above. Therefore, these two bands are probably associated with the vibrations of the O–H...O structures.

Table 1 shows the frequencies and damping constants used to fit the spectra of the $Li_{1-x}H_xIO_3$ crystal for $x = 0.32$, as well as the symmetry and assignments of the vibrational modes. The region of the spectra below 500 cm^{-1} corresponds to the external and bending internal modes (ν_2 and ν_4). Above 500 cm^{-1}, we found the stretching internal modes (ν_1 and ν_3), and those at about 590 and 730 cm^{-1} associated with the O–H...O structures.

In the $Y(XZ)\bar{Y}$ spectra (figure 3(c)), we found the $E_1(TO)$ and $E_1(LO)$ modes. All modes below 500 cm^{-1} have a weak polar character, and, thus, each peak corresponds to a superposition of the TO and LO modes. The assignment of these modes has been made in accordance to the assignment of those of $LiIO_3$ [11, 12]. The peaks below 400 cm^{-1} are associated with the external modes. The internal mode is ν_4 found at 441 cm^{-1} and the internal mode ν_2 could not be unambiguously identified in the spectrum. The attribution of the modes above 500 cm^{-1} is straightforward. The modes of the O–H...O structures have their frequencies at 586 and 726 cm^{-1}. The most polar internal mode (ν_3) has its TO and LO frequencies at 761 and 842 cm^{-1}. Note that they are close to those of the pure compound $LiIO_3$ [11–14]. The other two peaks are certainly associated with the (TO and LO) modes ν_1, which now appear in this configuration. Note that they appear between the ν_3-TO and LO frequencies. Therefore, the ν_1-LO mode must have a frequency smaller than that of the ν_1-TO mode. This is due to the fact that there is always a zero (a pole) between two poles (zeros) of the dielectric function.

The $A(LO)$ and E_2 modes are found in the $Z(XX)\bar{Z}$ spectra, and the $A(TO)$ and E_2 modes appear in the $Y(XX)\bar{Y}$ spectra. The attribution of the modes has also been made in accordance with those of the pure compound $LiIO_3$ [11, 12]. Moreover, the E_2 modes must appear in the two spectra with the same frequencies and damping constants. The external and internal bending modes (ν_2 and ν_4) appear below 500 cm^{-1}. Note that the bending internal modes respect the same selection rule as $LiIO_3$. The mode ν_4 belongs to the E_2 representation, and the longitudinal mode ν_2 belongs to the A representation. The ν_2-$A(TO)$

Table 1. Frequencies and damping constants used to fit the spectra of the $Li_{1-x}H_xIO_3$ ($x = 0.32$) single crystal in three scattering configurations, as well as the symmetries and assignments of the vibrational modes.

$Z(XX)\bar{Z}$				$Y(XX)\bar{Y}$			
Frequency (cm^{-1})	Damping (cm^{-1})	Symmetry and assignment		Frequency (cm^{-1})	Damping (cm^{-1})	Symmetry and assignment	
102	24	E_2	External	102	24	E_2	External
157	44	A(LO)	External	157	44	A(TO)	External
225	50	A(LO)	External				
328	44	E_2	External	328	44	E_2	External
344	28	E_2	ν_4	344	28	E_2	ν_4
449	58	A(LO)	ν_2				
590	50		O–H...O	590	50		O–H...O
731	56		O–H...O	731	56		O–H...O
766	34	E_2	ν_3	766	32	E_2	ν_3
				782	22	A(TO)	ν_1
801	28	A(LO)	ν_1				
820	24	E_2	ν_1	820	24	E_2	ν_1
839	24	A(LO)	ν_3				

$Y(XZ)\bar{Y}$			
Frequency (cm^{-1})	Damping (cm^{-1})	Symmetry and assignment	
94	64	$E_1(TO + LO)$	External
171	48	$E_1(TO + LO)$	External
304	22	$E_1(TO + LO)$	External
326	30	$E_1(TO + LO)$	External
441	62	$E_1(TO + LO)$	ν_4
586	48		O–H...O
726	48		O–H...O
761	32	$E_1(TO)$	ν_3
780	32	$E_1(LO)$	ν_1
807	36	$E_1(TO)$	ν_1
842	24	$E_1(LO)$	ν_3

mode could not be identified in the spectrum. The modes of the O–H...O structures now have their frequencies at 590 and 731 cm^{-1}. The most intense peaks above 500 cm^{-1} in the $Y(XX)\bar{Y}$ and $Z(XX)\bar{Z}$ spectra are at 782 and 801 cm^{-1}, respectively. Certainly, they correspond to the ν_1-A(TO) and ν_1-A(LO) modes, since the peaks associated with the totally symmetrical mode are always the most intense in the Raman spectra. The peak that appears at 766 cm^{-1} in both scattering geometries is certainly the ν_3-E_2 symmetry mode and the peak at 820 cm^{-1} is probably the ν_1-E_2 symmetry mode. The small peak at 839 cm^{-1} found in the $Z(XX)\bar{Z}$ spectra corresponds to a ν_3-A(LO) mode. The ν_3-A(TO) mode could not be unambiguously identified in the $Y(XX)\bar{Y}$ spectrum. Note that this mode is forbidden in the $Y(XX)\bar{Y}$ $LiIO_3$ spectrum, and, therefore, its intensity is expected to be very small in the present case.

4. Conclusion

In this work, we presented a complete polarized Raman study of $Li_{1-x}H_xIO_3$ single crystals, for several values of the proton concentration x, using different scattering geometries. The

Raman spectra of these solid solutions for x in the range $0.27 < x < 0.36$ are composed by broad bands associated with the internal modes of the iodate anions, the external and the librational modes. Two peaks centred at about 590 and 730 cm^{-1} that appear in all of the spectra are certainly associated with the presence of protons in the structure, and probably due to the vibrations of the O–H . . . O structures. The broad bands of the Raman spectra for different scattering geometries have been fitted in accordance with a group theoretical analysis, allowing us to assign the modes, and determine their frequencies and damping constants. The results show that the average symmetry of these crystals is hexagonal, similarly to the case for the pure compound α-LiIO$_3$. However, the random presence of protons in the structure breaks the C$_3$ symmetry of the iodate sites, thus changing the selection rules for the Raman scattering.

Acknowledgments

References

[1] Ricci J E and Amron I 1951 *J. Am. Chem. Soc.* **73** 3613
[2] De Boer J L, Van Bolhuis F, Olthaf-Hazekamp R and Vos A 1966 *Acta Crystallogr.* **21** 841
[3] Rogers M T and Helmholtz L 1941 *J. Am. Chem. Soc.* **63** 278
[4] Hamid S A and Kunze G 1977 *Acta Crystallogr.* A **33** 264
[5] Avdienko K I, Kostritskii S M, Kotlyarov V V and Semenov A E 1985 *Sov. Phys.–Solid State* **27** 2217
[6] Barabash A I, Gravilko T A, Petrosyan A M, Puchkovskaya G A and Roshchin A N 1991 *Bull. Acad. Sci. USSR Ser. Fiz* **55** 94
[7] Le Roy J, Crettez J M, Coquet E and Bouillot J 1990 *Solid State Commun.* **75** 539
[8] Le Roy J, Rosso C, Bouillot J, Crettez J M, Boucherle J X and Bonnet M 1995 *J. Solid State Chem.* **115** 309
[9] Bouillot J, Coquet E, Pannetier J and Crettez J M 1986 *Physica* B **136** 493
[10] Oliveira M A S 1995 *Master's Thesis* Departamento de Fisica, Universidade Federal de Minas Gerais, Belo Horizonte, Brazil
[11] Crettez J M, Misset J P and Coquet E 1979 *J. Chem. Phys.* **70** 4194
[12] Cerdeira F, Lemos V, Melo F E A and Cardona M 1984 *Phys. Status. Solidi* b **122** 53
[13] Otaguro W, Wiener-Avnear E, Aguello C A and Porto S P S 1971 *Phys. Rev.* B **4** 4542
[14] Melo F E A, Cerdeira F and Lemos V 1982 *Solid State Commun.* **41** 281
[15] Turrel G 1972 *Infrared and Raman Spectra of Crystals* (London: Academic)